A correction procedure for characteristic fluorescence encountered in microprobe analysis near phase boundaries

SCANNING Vol. 5, 172–183 (1983)

Received: February 21st, 1983

Original Paper

A Correction Procedure for Characteristic Fluorescence Encountered in Microprobe Analysis near Phase Boundaries

G. F. Bastin, F. J. J. van Loo, P. J. C. Vosters and J. W. G. A. Vrolijk

Laboratory for Physical Chemistry, Eindhoven University of Technology, P. O. Box 513, 5600 MB Eindhoven, Netherlands

Introduction

When dealing with the problem of spatial resolution in quantitative electron probe micro-analysis it is usually the electron range people are first concerned about. This electron range can be defined as the distance the electrons diffuse away from the point of impact of the electron beam on the specimen until they have lost so much energy as to be no longer capable of exciting primary characteristic x-radiation.

Typically this range is of the order of 1–2 μm yielding a volume of primary excitation of approximately 2–4 μm diameter. In many cases, however, the characteristic primary x-radiation of one or more of the elements in the specimen is powerful enough to excite one or more other elements, thus giving rise to enhanced x-ray production. The main trouble with this secondary production is that it usually takes place in a much larger volume. As a consequence the spatial resolution can be drastically lowered. As *Green* (1964) has shown, the volume in which secondary x-rays are produced, can be one to two orders of magnitude greater than the volume of primary production. The reason for this large difference is the fact that in general x-rays can travel much more easily through matter than electrons can. For the case of K-K fluorescence (Kα-radiation of one element exciting Kα-radiation of the other) the excitation of secondary radiation is especially bad in targets containing elements with atomic numbers differing by two (for atomic numbers $Z > 21$), like combinations of the elements Fe/Ni, Cu/Co etc. As these metals play a major role in our investigations of diffusion couples and phase diagrams we are frequently confronted with the problem of "fluorescence uncertainty" near phase boundaries and in small particles.

The situation is particularly bad when analysing for a low concentration of an element in a particle surrounded by a matrix containing large amounts of another element capable of exciting the first.

In such conditions dramatic errors in the analysis can be made as will be demonstrated. In the past the problem of fluorescence has been successfully dealt with by *Reed* (1965), *Reed* and *Long* (1963), *Henoc* et al. (1968), *Maurice* et al. (1965) and others. Especially the approach of *Reed* (1965, 1975) has led to the adoption of a fluorescence correction scheme which is now generally applied in ZAF correction procedures. One should, however, bear in mind that in this procedure it is implicitly assumed that the primary and secondary production of x-rays as well as the subsequent absorption, all take place in the same homogeneous matrix; a condition which to an increasing extent is violated as the electron beam approaches a phase boundary or when the size of a particle decreases below a certain limit. What would be needed in such cases is a correction procedure which gives a correction factor as a function of distance from the phase boundary (or of particle size).

It is immediately obvious that such a factor can only be calculated if certain assumptions are made about the geometry involved and, what is perhaps even more important, with a knowledge of the compositions on both sides of the interface, which are in fact the quantities to be measured! Hence the procedure is bound to be iterative in nature, like the ZAF correction procedure itself is.

We have developed such a procedure and applied it successfully to a number of concentration profiles in the Cu/Co, Cu/Co/O, Fe/Ni/O and similar systems. The theoretical approach we have chosen is essentially the one followed by *Maurice* et al. (1965) and later by *Henoc* (1968). Their rather rigorous treatment of the matter has led to equations which are well capable of predicting the apparent concentration of one element in the other as a function of distance in undiffused couples of pure metals with straight boundaries. By following their approach a few steps further similar equations can be derived for the general case of alloys joined together (diffusion couples) with straight or curved boundaries, small particles and lamellae, as will be shown.

Theory

In the following treatment it will be assumed that all primary radiation is emitted from a point source O located at the surface of the specimen, i. e. the point of impact of the electron beam. This assumption will considerably facilitate the calculations. Of course, an error will be made by not taking into account that, in fact, the x-ray distribution should be taken as a function of depth. However, the error involved is small as demonstrated by *Maurice* (1965). Moreover, as already assumed by *Castaing* (1955) and shown by *Maurice* et al. (1965) we can safely neglect that part of the primary radiation which is directed towards the surface as only the deeper layers of the specimen yield significant contributions to the emitted fluorescent radiation.

A last restriction must be made on the continuum fluorescence which has not been taken into account in the calculations as these are usually lengthy. In some cases estimates on this effect have been used.

The case of two homogeneous alloys separated by a straight boundary

Let us consider the case of two homogeneous alloys (Fig. 1) composed of the elements A and B in which $Z_B > Z_A$ and B Kα-radiation is capable of exciting A Kα-radiation. The electron beam is located at the surface of alloy LB (richest in B) at a distance d from the straight interface separating it from LA (richest in A). The x-rays are supposed to be taken off in a plane parallel to the interface (see Fig. 1). The intensity of

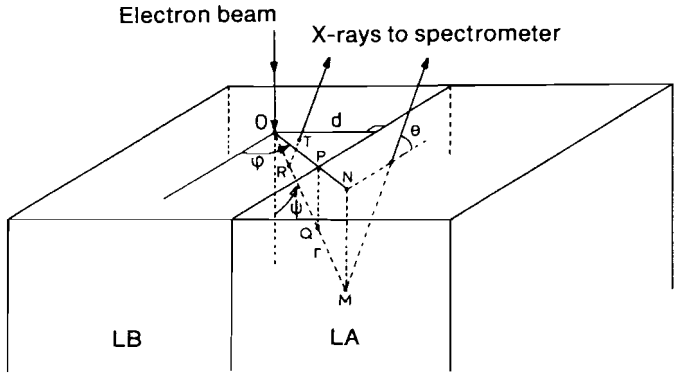

Fig. 1 Schematic drawing representing two alloys LB and LA seperated by a straight interface. The electron beam is located at a distance d from the boundary.

the primary B-radiation, I_B, emitted towards the interface into the solid angle delimited by the spherical coordinates ψ and $\psi + d\psi$ and Φ and $\Phi + d\Phi$ can be written as $I_B \sin\psi \, d\psi \, d\Phi/4\pi$.

On its way towards M this radiation is absorbed in two ways:
- up to Q in alloy LB (concentrations C_A^{LB}, C_B^{LB})
- subsequently, after crossing the interface, in alloy LA (concentrations C_A^{LA}, C_B^{LA}).

For the trajectory OQ the intensity as a function of distance r can be represented by:

$$I_B(OQ) = I_B \frac{\sin\psi d\psi d\Phi}{4\pi} \exp(-\mu_B^{LB} \varrho_{LB} r) \quad (1)$$

in which μ_B^{LB} is the mass absorption coefficient for B-Kα-radiation in alloy LB and ϱ_{LB} is the density of LB. Along this way both A- and B-atoms absorb part of the radiation according to:

$$dI = I_B(OQ) \, \mu_B^{LB} \, \varrho_{LB} \, dr.$$

A fraction hereof, equal to $C_A^{LB} \mu_B^A / \mu_B^{LB}$ is specifically absorbed by A-atoms and this fraction, in turn, is partly transformed into A-Kα fluorescent radiation according to:

$$dI_A^F(OQ, \text{exc.}) = \omega_A \left(\frac{r-1}{r}\right)_A \frac{C_A^{LB} \mu_B^A}{\mu_B^{LB}} \mu_B^{LB} \varrho_{LB} I_B(OQ) \, dr \quad (2)$$

in which ω_A is the fluorescent yield and $\left(\frac{r-1}{r}\right)_A$ is the absorption edge jump ratio for element A.

Combination of (1) and (2) yields for the excited fluorescent A-radiation along OQ:

$$dI_A^F(OQ, \text{exc.}) = I_B \frac{\sin\psi d\psi d\Phi}{4\pi} \omega_A \left(\frac{r-1}{r}\right)_A C_A^{LB} \mu_B^A \varrho_{LB} \times \exp(-\mu_B^{LB} \varrho_{LB} r) \, dr \quad (3)$$

with $0 \leq r < d/\sin\psi \sin\Phi$.

In order to be "seen" by the spectrometer this radiation has to emerge (for example from R in T) under an angle Θ, thereby passing the trajectory RT in LB with simultaneous absorption according to a factor:

$$\exp(-\mu_A^{LB}\,\varrho_{LB}\,r\cos\psi\,\mathrm{cosec}\,\Theta).$$

In total we get between O and d/sinψ sinΦ for each increment dr an amount of *emitted* fluorescent A-radiation of:

$$dI_A^F(OQ) = I_B\,\frac{\omega_A}{4\pi}\,(\frac{r-1}{r})_A\,C_A^{LB}\,\mu_B^A\,\varrho_{LB}\times$$

$$\exp(-\mu_B^{LB}\,\varrho_{LB}\,r - \mu_A^{LB}\,\varrho_{LB}\cos\psi\,\mathrm{cosec}\,\Theta\,r)\,dr\sin\psi d\psi d\Phi.$$

In order to obtain the total amount emitted from LB between O and the boundary this expression has to be integrated over r (from 0 to d/sinψ sinΦ), ψ (from 0 to $\pi/2$) and Φ (from 0 to π).

After the integration has been carried out over r we get for the part of the fluorescent A-radiation which is excited by primary B-radiation directed towards the interface (i.e. $0<\Phi<\pi$):

$$I_A^F(0<\Phi<\pi) = \frac{\omega_A}{4\pi}\,(\frac{r-1}{r})_A\,C_A^{LB}\,\mu_B^A\,I_B\times$$

$$\int_{\Phi=0}^{\pi}\int_{\psi=0}^{\pi/2}\sin\psi d\psi d\Phi\times \qquad (4)$$

$$\left[\frac{1-\exp\{-(\mu_B^{LB}\,\varrho_{LB}+\mu_A^{LB}\,\varrho_{LB}\cos\psi\,\mathrm{cosec}\Theta)\,d/\sin\psi\sin\Phi\}}{\mu_B^{LB}+\mu_A^{LB}\cos\psi\,\mathrm{cosec}\Theta}\right] \qquad (4)$$

In order to obtain the total amount of fluorescent A-radiation emitted from LB we have to add the contribution produced by the part of primary B-radiation which is directed towards the left, away from the interface ($\pi<\Phi<2\pi$). This contribution can be calculated by integration over r (with $0<r<\infty$), Φ(with $\pi<\Phi<2\pi \equiv 0<\Phi<\pi$) and ψ (with $0<\psi<\pi/2$):

$$I_A^F(\pi<\Phi<2\pi) = \frac{\omega_A}{4\pi}\,(\frac{r-1}{r})_A\,C_A^{LB}\,\mu_B^A\,I_B\times$$

$$\int_{\Phi=0}^{\pi}\int_{\psi=0}^{\pi/2}\frac{\sin\psi\,d\psi\,d\Phi}{\mu_B^{LB}+\mu_A^{LB}\cos\psi\,\mathrm{cosec}\Theta}$$

Thus we get for the total amount of fluorescent A-radiation emitted from LB:

$$I_A^F(LB) = \frac{\omega_A}{4\pi}\,(\frac{r-1}{r})_A\,\mu_B^A\,C_A^{LB}\,I_B\times$$

$$\int_{\Phi=0}^{\pi}\int_{\psi=0}^{\pi/2}\frac{\sin\psi\,d\psi\,d\Phi}{\mu_B^{LB}+\mu_A^{LB}\cos\psi\,\mathrm{cosec}\Theta}\times$$

$$\left[2-\exp\{-(\mu_B^{LB}\,\varrho_{LB}+\mu_A^{LB}\,\varrho_{LB}\cos\psi\,\mathrm{cosec}\Theta)\,d/\sin\psi\sin\Phi\}\right] \qquad (5)$$

Now it remains to determine the ratio I_A/I_B of the primarily excited A-Kα and B-Kα-intensities in order to calculate the ratio I_A^F/I_A which is actually required for correction.

Therefore we use the equation proposed by *Green* and *Cosslett* (1961) and modified by *Reed* and *Long* (1963):

$$\frac{I_B}{I_A} = \frac{C_B}{C_A}\,\frac{\omega_K(B)}{\omega_K(A)}\,\frac{A_A}{A_B}\left(\frac{U_B-1}{U_A-1}\right)^{5/3}$$

in which A denotes the atomic weight and U the so-called overvoltage (accelerating voltage/critical excitation voltage). Substitution in (5) yields:

$$\frac{I_A^F}{I_A}(LB) = S\,C_B^{LB}\int_{\Phi=0}^{\pi}\int_{\psi=0}^{\pi/2}\frac{\sin\psi\,d\psi\,d\Phi}{\mu_B^{LB}+\mu_A^{LB}\cos\psi\,\mathrm{cosec}\Theta}$$

$$\times\left[2-\exp\{-(\mu_B^{LB}\,\varrho_{LB}+\mu_A^{LB}\,\varrho_{LB}\cos\psi\,\mathrm{cosec}\Theta)\times d/\sin\psi\sin\Phi\}\right] \qquad (6)$$

$$\text{with } S = \frac{\omega_B}{4\pi}\left(\frac{r-1}{r}\right)_A\frac{A_A}{A_B}\mu_B^A\left(\frac{U_B-1}{U_A-1}\right)^{5/3}$$

It will be noted here that, when d goes to infinity this equation automatically transforms into the Reed equation for the fluorescence correction in a homogeneous matrix, apart from a small term which corrects for the depth at which the primary excitation is excited. Now let us turn back to the trajectory OM in order to calculate the amount of fluorescent A-radiation emitted from LA, across the boundary.

After travelling the distance OQ through LB the original intensity I_B is decreased to:

$$I_B\,\frac{\sin\psi\,d\psi\,d\Phi}{4\pi}\exp(-\mu_B^{LB}\,\varrho_{LB}.d/\sin\psi\sin\Phi).$$

From then on attenuation takes place according to:

$$\exp(-\mu_B^{LA}\,\varrho_{LA}\,r) \text{ with } d/\sin\psi\sin\Phi<r<\infty.$$

Following the same line of reasoning as before we eventually arrive at:

$$\frac{I_A^F}{I_A(LA)} = S\,\frac{C_B^{LB}\,C_A^{LA}}{C_A^{LB}}\int_{\Phi=0}^{\pi}\int_{\psi=0}^{\pi/2}\frac{\sin\psi\,d\psi\,d\Phi}{\mu_B^{LA}+\mu_A^{LA}\cos\psi\,\mathrm{cosec}\Theta}$$

$$\exp\{-(\mu_B^{LB}\,\varrho_{LB}+\mu_A^{LA}\,\varrho_{LA}\cos\psi\,\mathrm{cosec}\Theta)\,d/\sin\psi\sin\Phi\} \qquad (7)$$

in which S has the same meaning as before.

Ultimately the total ratio of fluorescent to primary radiation ist obtained by adding the contributions according to (6) and (7). This ratio can now be used to correct the measured k-ratio for fluorescence by multiplying it with $1/(1 + I_A^F/I_A)$.

The case of two pure elements separated by a straight interface parallel to the electron beam can be considered as a special case of the foregoing problem in which there is no contribution from LB (≡ pure B). Furthermore, there is, of course, no excitation of primary A-radiation within LB. Therefore the amount

of fluorescent A-radiation has to be calculated with respect to the intensity produced in pure A, thus yielding the k-ratio or apparent concentration of A in B.

Equation (7) then reduces to:

$$k_A = \frac{I_A^F}{I_{A,\,pure}} = S \int_{\Phi=0}^{\pi} \int_{\psi=0}^{\pi/2} \frac{\sin\psi \, d\psi \, d\Phi}{\mu_B^A + \mu_A^A \cos\psi \operatorname{cosec}\Theta} \exp\{-(\mu_B^B \varrho_B + \mu_A^A \varrho_A \cos\psi \operatorname{cosec}\Theta) \, d/\sin\psi \sin\Phi\}. \quad (8)$$

This is exactly the equation derived by *Henoc* et al. (1968). Another interesting geometry with possible practical application is that of a lamella with thickness 2d (other dimensions very large) which is irradiated in its centre (see Fig. 2a).

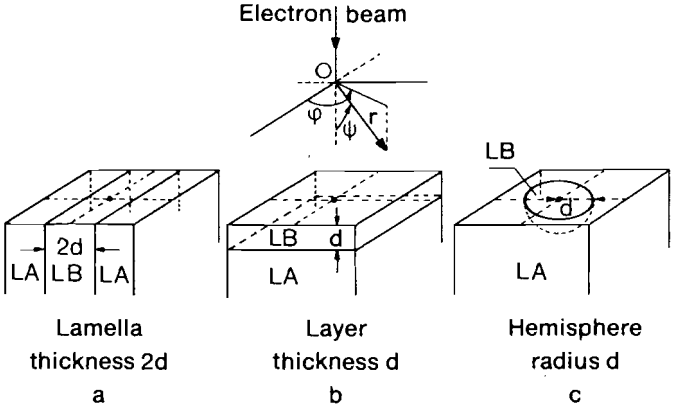

Fig. 2 Schematic drawings representing the case of: (a) a lamella (thickness 2d); (b) a layer (thickness d) on top of a substrate; (c) a hemisphere (radius d).

In this case it can easily be seen that the total amount of emitted fluorescent A-radiation is obtained by adding twice the amount calculated by equation (4) and twice the amount calculated by (7) thus yielding:

$$\frac{I_A^F}{I_A}(LB) = 2\,S\,C_B^{LB} \int_{\Phi=0}^{\pi} \int_{\psi=0}^{\pi/2} \frac{\sin\psi \, d\psi \, d\Phi}{\mu_B^{LB} + \mu_A^{LB} \cos\psi \operatorname{cosec}\Theta} \times [1-\exp\{-(\mu_B^{LB} \varrho_{LB} + \mu_A^{LB} \varrho_{LB} \cos\psi \operatorname{cosec}\Theta) \, d/\sin\psi \sin\Phi\}] \quad (9)$$

$$\frac{I_A^F}{I_A}(LA) = 2\,S \frac{C_B^{LB} C_A^{LA}}{C_A^{LB}} \int_{\Phi=0}^{\pi} \int_{\psi=0}^{\pi/2} \frac{\sin\psi \, d\psi \, d\Phi}{\mu_B^{LA} + \mu_A^{LA} \cos\psi \operatorname{cosec}\Theta} \times \exp\{-(\mu_B^{LB} \varrho_{LB} + \mu_A^{LA} \varrho_{LA} \cos\psi \operatorname{cosec}\Theta) \, d/\sin\psi \sin\Phi\} \quad (10)$$

with S having the same meaning as before.

A last case which can be conceived with straight boundaries and of possible interest for practical purposes is that of a thin layer (thickness d) of alloy LB on top of a substrate LA (see Fig. 2b).

The only difference with the foregoing cases is that now radial symmetry with respect to the incident beam is present and that the integration over r has to take place from 0 to d/cos ψ (for the fraction emitted from LB) and from d/cos ψ to ∞ (for the fraction emitted from the substrate LA). Furthermore the integration over Φ takes place for $0<\Phi<2\pi$ which in this case simply means multiplying with 2π.

The difference in absorption for the emerging fluorescent A-radiation from the substrate between LA and LB is neglected. This will not introduce a large error as, contrary to B-radiation, the mass absorption coefficient for A-radiation will not greatly differ between LA and LB. Anyhow, the majority of absorption takes place in LA. We will get therefore:

$$\frac{I_A^F}{I_A}(LB) = 2\pi\,S\,C_B^{LB} \int_{\psi=0}^{\pi/2} \frac{\sin\psi \, d\psi}{\mu_B^{LB} + \mu_A^{LB} \cos\psi \operatorname{cosec}\Theta} \times [1-\exp\{-(\mu_B^{LB} \varrho_{LB} + \mu_A^{LB} \varrho_{LB} \cos\psi \operatorname{cosec}\Theta) \, d/\cos\psi\}] \quad (11)$$

and:

$$\frac{I_A^F}{I_A}(LA) = 2\pi\,S \frac{C_B^{LB} C_A^{LA}}{C_A^{LB}} \int_{\psi=0}^{\pi/2} \frac{\sin\psi \, d\psi}{\mu_B^{LA} + \mu_A^{LA} \cos\psi \operatorname{cosec}\Theta} \times \exp\{-(\mu_B^{LB} \varrho_{LB} + \mu_A^{LA} \varrho_{LA} \cos\psi \operatorname{cosec}\Theta) \, d/\cos\psi\} \quad (12)$$

It will be noted that also for the last two cases for large values of d a close approximation of the Reed correction equation is obtained.

The case of two homogeneous alloys separated by a curved boundary

The model which has been chosen in this case is that of a hemisphere of alloy LB embedded in a matrix of LA and which is irradiated in its centre. Let the radius of the hemisphere be d (see Fig. 2c). Due to the spherical symmetry involved integration in this case is even easier than before: Integration over r takes place over 0 to d, and d to ∞, respectively. Eventually we arrive at:

$$\frac{I_A^F}{I_A}(LB) = 2\pi\,S\,C_B^{LB} \int_{\psi=0}^{\pi/2} \frac{\sin\psi \, d\psi}{\mu_B^{LB} + \mu_A^{LB} \cos\psi \operatorname{cosec}\Theta} \times [1-\exp\{-(\mu_B^{LB} \varrho_{LB} + \mu_A^{LB} \varrho_{LB} \cos\psi \operatorname{cosec}\Theta) \, d\}] \quad (13)$$

and:

$$\frac{I_A^F}{I_A}(LA) = 2\pi S \frac{C_B^{LB} C_A^{LA}}{C_A^{LB}} \int_{\psi=0}^{\pi/2} \frac{\sin\psi \, d\psi}{\mu_B^{LA} + \mu_A^{LA} \cos\psi \operatorname{cosec}\Theta}$$

$$\times \exp\{-(\mu_B^{LB} \varrho_{LB} + \mu_A^{LA} \varrho_{LA} \cos\psi \operatorname{cosec}\Theta) d\} \quad (14)$$

Some general remarks on the equations derived

Although the complexity of the equations derived prevents an easy insight into the practical consequences some general conclusions can yet be drawn. First there is the rather discouraging fact that there is little to be changed in the experimental conditions in order to reduce the effect of secondary fluorescence: For a given alloy system and geometry and a given microprobe (fixed take-off angle) the only quantity to be chosen is $\left(\frac{U_B-1}{U_A-1}\right)^{5/3}$, contained in S.

Unfortunately this factor does not change rapidly enough in the range of overvoltages most analyses are performed in ($1.5<U<2.5$); e.g. in the Cu/Co system this factor varies between 0.51 (for $U_{Cu} = 1.5$) to 0.67 (for $U_{Cu} = 2.5$). A fast change is only realised by reducing the accelerating voltage until just above the critical excitation voltage for Cu, but clearly this would not be practicable for a number of reasons.

The second observation is that, as one would imagine, the concentrations of both elements in the adjoining alloys play a crucial role. The problems increase with increasing concentration of A in LA and B in LB.

The next interesting question would be which of the geometries discussed would need the largest amount of correction for a given value of the parameter d; in other words, which is the worst case. For a full answer the equations have to be solved for a given set of conditions which, nowadays, with modern computers, presents no problem at all. Even without solving the integrals it can be demonstrated that the first case is the most and the last case the least favourable; by considering the limiting cases for which d goes to zero. For simplicity we will assume that two pure elements A and B are joined together. As the exponential term in equation (8) assumes the value 1 it follows that: k_A = S times π times (integral over ψ only).

In all other cases k_A will be equal to twice this amount for d approaching zero. For increasing values of d it can be seen that the amount of correction needed decreases most rapidly in the case of one straight boundary (Fig. 1 and eqs. (6) and (7)) as d in the exponential term is divided by sin ψ and sin Φ, thus increasing the exponent. In equations (11) and (12) d is divided by cos ψ whereas in eqs. (13) and (14) d is not divided at all, thus giving rise to a slower and slower decrease in emitted fluorescent radiation with increasing parameter d. This effect can also be conceived by imagining the originally straight interface in Fig. 1 slowly being curved around 0. It is apparent that all parts of alloy LA represented by either small (close to zero) or large (close to π) values of Φ, which normally play no significant role, gradually start to add substantial contributions to the emitted fluorescent radiation. When a similar procedure is applied to the left hand side of 0 and also below the suface, the situation of a hemisphere is gradually obtained. So it can be imagined that this geometry represents definitely the worst case. Unfortunately this is a kind of geometry which, by approximation, is frequently encountered in microprobe analysis and it is suspected that many people do not sufficiently realise the adverse effects fluorescence can have on the quality of their measurements especially when low concentrations of an element "suffering" from secondary excitation are being analysed in small particles surrounded by a matrix containing large concentrations of this element.

Some Examples of Calculations and some Tests

Fig. 3 shows the calculated results as a function of the parameter d for the two limiting geometries straight boundary vs. hemisphere for the case of pure Cu and Co. The calculations have been performed for an accelerating voltage of 20 kV and a take-off angle of 40°.

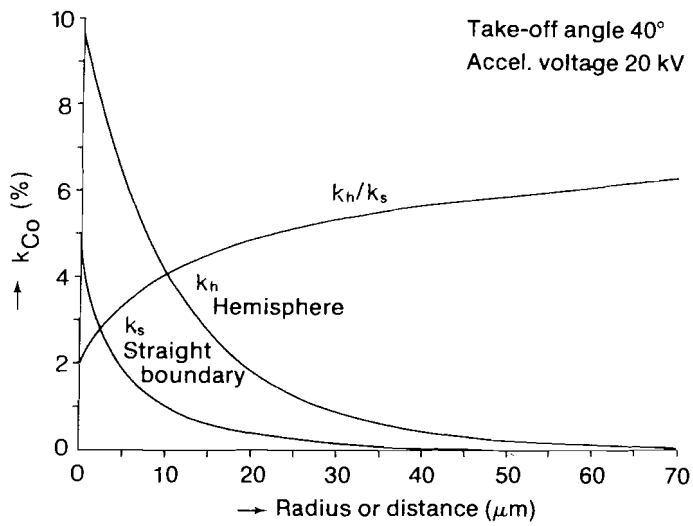

Fig. 3 Comparison between the apparent k-ratio k_s for Co in Cu as a function of distance from a straight interface Cu/Co and the apparent k-ratio for Co (k_H) as a function of the radius of a Cu-hemisphere in a pure Co matrix. Also shown is the ratio k_H/k_s. Take-off angle 40°; acc. voltage 20 kV.

It is obvious that the apparent k-ratio for Co Kα-radiation decreases much faster in the case of a straight boundary than for a hemisphere. The ratio between the apparent k-values calculated for the two geometries shows a variation between 2 (for d approaching zero) and more than 6 (for large values of d). For take-off angles smaller than 40° the situation is slightly more, for angles larger than 40° slightly less favourable. The rather dramatic consequences for the case of the hemisphere are perhaps even better illustrated in Fig. 4a where, again for the Cu-Co system, the ratio between the apparent k-value for Co obtained from a hemisphere with varying radius d and the k-value for an infinitely large hemisphere has been plotted for various concentrations. The composition of the hemisphere has been varied between 1 and 20 wt% Co, balance Cu; the composition of the matrix has been fixed at Co-10 wt% Cu. From Fig. 4a it follows, for example, that for a radius of 5 μm and a Co-content of 1% an apparent concentration of more than 5% would be measured! The reason for this effect must be sought in the fact that for low Co-concentrations the particle is relatively transparent for the Cu Kα-X-rays (m.a.c. in pure Cu = 53 cm²/g), which will easily leave the particle and excite the matrix. With increasing Co-content the m.a.c. increases fast (m.a.c. in Co = 348 cm²/g!) and more secondary Co-radiation will be produced inside the particle itself. This is demonstrated in Fig. 4b where the ratio of fluorescent Co Kα radiation emitted from inside the particle to the totally emitted fluorescent Co Kα radiation has been plotted versus d. It is evident that for a Co-content of 1% one needs already a radius of about 40 μm to produce just as much within the particle as in the matrix.

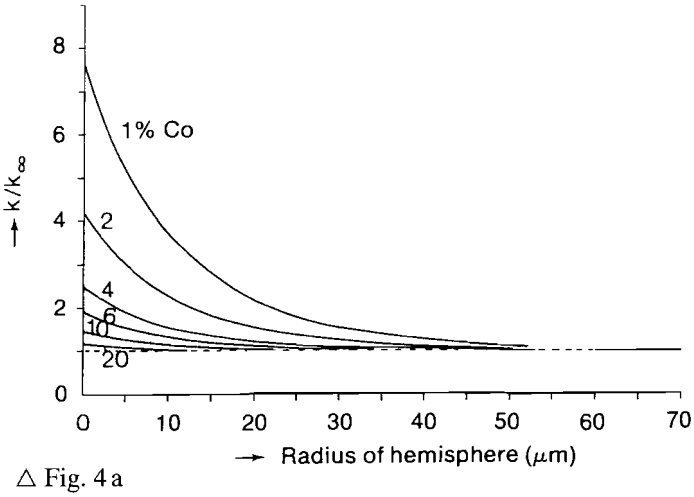

△ Fig. 4a

Fig. 4 b ▽

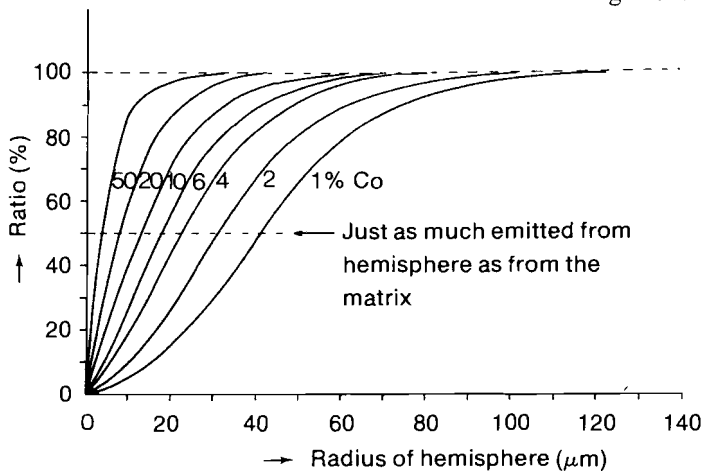

Fig. 4 (a) The apparent k-ratio for Co in a Cu-hemisphere, containing varying concentrations of Co, embedded in a matrix of fixed composition Co-10wt%Cu, as a function of the radius of the hemisphere. The k-ratios have been related to the value (k∞) which would have been measured in an infinitely large hemisphere.
(b) The fraction of fluorescent Co Kα-radiation emitted from the hemisphere in (a) in relation to the total amount emitted (hemisphere + matrix). The composition of the matrix is fixed at Co(10 wt%Cu).

We have now come to a stage where we would like to test some of the equations derived. As the case of the hemisphere is difficult to realize in a practical test we have chosen for the model with one straight boundary (Fig. 1). Although many combinations of pure metals and some alloys have been measured, we will limit ourselves to some results of the Cu-Co system (see Fig. 5).

This couple was prepared by clamping Cu and Co together in a vice, followed by sectioning and careful polishing of the complete assembly. The electron probe measurements were performed on a JEOL Superprobe 733 (takeoff angle 40°; acc. voltage 20 kV).

As Fig. 5 shows the shape of the calculated curve (open circles) corresponds very well with that of the measured curve (crosses) although all calculated values are somewhat low. Most probably this is due to the fact that the contribution of fluorescence by the continuum has been neglected, which, especially for small values of d, should give differences between the calculated and measured values.

On the right hand side of Fig. 5 the measured apparent Cu-concentration in Co has been plotted which must be due to continuum fluorescence. This curve can (for d > 3 μm) well be represented by:

$k_{Cu} = 1.35 \exp(-0.143\ d)$ (k in %; d in μm).

If a similar curve is assumed for the left hand side of Fig. 5 and the corresponding contribution added to the value calculated for K-K fluorescence, then the solid circles are obtained which show excellent agreement with the measured curve.

The same test has been performed with a number of equilibrated Cu(Co) alloys with different compositions which had been joined without diffusion to a Co (4.1 wt% Cu) alloy (see Fig. 6).

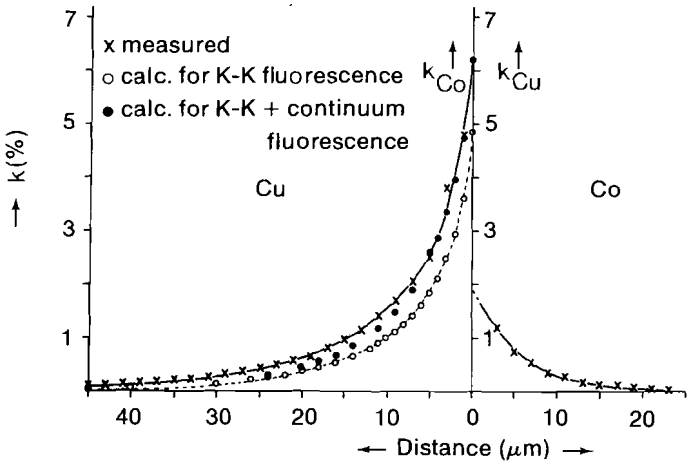

Fig. 5 The apparent k-ratio for Co in Cu (left hand side) as a fuction of distance in an undiffused Cu/Co couple: measured (crosses), calculated for K-K fluorescence only (open circles) and calculated for K-K fluorescence + estimated continuum fluorescence (solid circles). On the right hand side the apparent k-ratio for Cu in Co has been plotted. This can be represented by $k_{Cu} = 1.35 \exp(-0.143\ d)$ (k in %; d in μm).

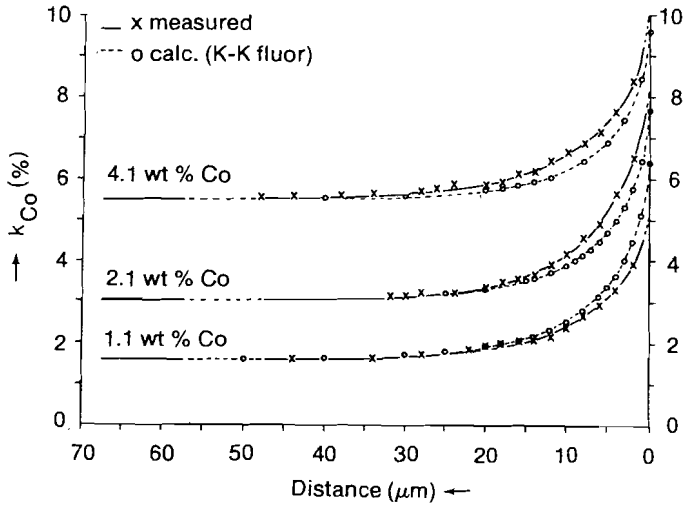

Fig. 6 Apparent k-ratio for Co in three different homogeneous Cu(Co) alloys as a function of distance from the straight boundary with a Co (4.1 wt% Cu) alloy. The measured and calculated values are represented by crosses and open circles, respectively.

Considering the fact that in these examples the effects of continuum fluorescence have been neglected the agreement between the calculated and measured values can be called quite satisfactory.

The Suggested Correction Procedure

As Figs. 3–6 have clearly demonstrated the need for a fluorescence correction procedure which gives the correction factor as a function of distance, or particle size (or in general the parameter d) is obvious. However, as we have pointed out in the introduction, such a correction factor can only be calculated for a given geometry with a knowledge of the concentrations on both sides of the interface. As these are at the same time the quantities to be measured it is inevitable that the correction procedure is iterative in nature. In the following we will briefly outline our correction procedure for which again the Cu/Co system will serve as an example:

a) Using the normal ZAF correction program the electron probe measurements (k-ratios for Co and Cu) as a function of distance are converted into concentrations for both sides of the interface.

b) Using the calculated concentrations (which on the low-Co side will be inevitably too high in Co) an estimate is made of the average Co-concentration C_A^{LB} over a region of 5–25 μm away from the boundary on the low-Co side of the couple. Of course the limits of 5 and 25 μm seem rather arbitrary.

The 5 μm limit has been chosen to exclude most of the continuum fluorescence effects; the high limit corresponds approximately with the distance the K-K-fluorescence effect is noticeable (see Figs. 5 and 6). With respect to the high-Co side an average concentration can well be calculated as in this part of the couple the measurements are hardly hampered by fluorescence. Moreover, calculations have shown that this concentration is not so critical. Therefore we will hold this concentration fixed during the rest of the procedure.

c) Next the originally measured k-value for Co on the low-Co side are corrected with fluorescence correction factors F(d), equal to $1/[1 + I_A^F/I_A\ (\text{total})]$, which have been calculated as a function of d according to equations (6) and (7) using the estimated average concentrations C_A^{LB} and C_A^{LA}.

d) Then the fluorescence correction in the ZAF program is disabled and the corrected k-values for Co and the original k-values for Cu submitted to the atomic number and absorption correction procedures of the ZAF program

e) The new concentration profile is subsequently used to generate a new estimate of C_B^{LB} while C_A^{LA} is still kept fixed.

f) With the new value of C_A^{LB} a new set of F(d) values is calculated and steps (c)–(e) are repeated. This will yield a lower value for C_A^{LB} for each iteration. The iterations are stopped as soon as the new estimate for C_A^{LB} differs less than, say, 0.05 wt% from the previous estimate, provided, of course, that convergence occurs. According to our experience so far, however, this has never failed and in the majority of cases the stopping criterion has been reached in 2 or 3 steps.

We will first test this procedure on some of the undiffused examples in Fig. 6 from which we know there should be no concentration gradient, of course. We will assume C_A^{LA} to be known and equal to 95.9 wt% Co (4.1 wt% Cu) which, as we have discussed before, would have been measured anyway. In Fig. 7 the concentration profiles (crosses) for two of the couples from Fig. 6 have been plotted as they have been obtained through the ZAF correction program. One of them, namely the Cu–1.1 wt% Co/Co–4.1 wt% Cu couple (lower part of Fig. 7) will now be discussed in detail.

It is obvious that without a specific correction for fluorescence a boundary concentration of about 3.5 wt% Co would have been measured which goes to show again how big the errors are that can be made. For the first iteration an initial value of 2% Co has been chosen for C_A^{LB}. This is somewhat higher than the average value of 1.5% but for the first iteration this does not really matter much.

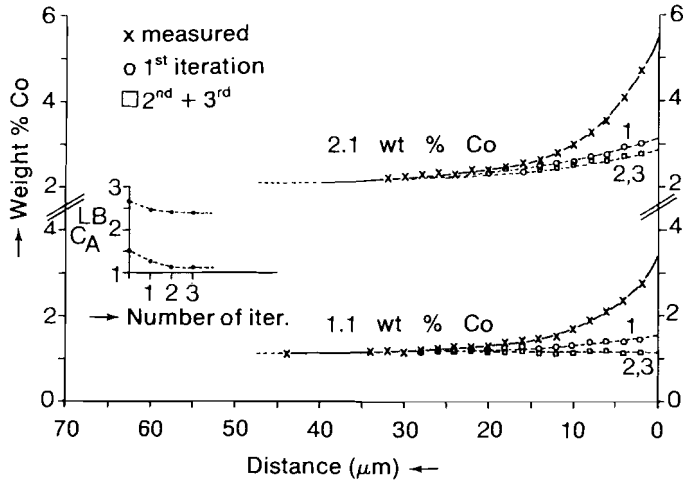

Fig. 7 The proposed iteration procedure applied to two of the three examples in Fig. 6. The measured values are designated by crosses, the results for the various iterations by open symbols. On the left hand side the average value of C_A^{LB} over 5–25 μm from the boundary is shown for each iteration.

The first calculation leads to the F(d)-values shown in Table 1. Note the large differences between these values and the F-values generated by the ZAF program, which are constantly about 0.7. Also note that for large values of d there is about 5–6% undercorrection in our model, due to the fact that the second logarithmic term in the Reed correction term, which contains the Lenard coefficient σ, has been left out.

Table 1 Results for the undiffused test couple Cu(1.1wt%Co) / Co(4.1wt%Cu)

	Measured values			1st Iter. 2%		2nd Iter. 1.3%		3rd Iter. 1.13%	
d (m)	k_{Co}(%)	C_{Co}(wt%)	F*	F(d)	C_{Co}(wt%)	F(d)	C_{Co}(wt%)	F(d)	C_{Co}(wt%)
2	3.868	2.75	0.716	0.380	1.44	0.295	1.11	0.283	1.09
4	3.295	2.33	0.713	0.443	1.40	0.350	1.11	0.340	1.11
6	2.918	2.06	0.711	0.493	1.42	0.405	1.17	0.390	1.13
8	2.660	1.87	0.709	0.535	1.38	0.450	1.16	0.436	1.15
10	2.375	1.67	0.708	0.569	1.30	0.485	1.11	0.480	1.13
12	2.138	1.50	0.707	0.598	1.25	0.522	1.09	0.513	1.18
14	2.081	1.46	0.706	0.621	1.23	0.560	1.12	0.546	1.13
16	2.034	1.43	0.706	0.641	1.27	0.580	1.15	0.572	1.15
18	1.994	1.40	0.706	0.657	1.24	0.605	1.14	0.595	1.18
20	1.857	1.30	0.705	0.671	1.20	0.625	1.12	0.616	1.13
22	1.845	1.29	0.705	0.685	1.22	0.643	1.15	0.635	1.16
24	1.812	1.27	0.705	0.695	1.24	0.658	1.17	0.650	1.17
26	1.776	1.24	0.705	0.702	1.18	0.670	1.13	0.663	1.17
28	1.716	1.20	0.704	0.708	1.19	0.678	1.14	0.673	1.14
30	1.631	1.14	0.704	0.712	1.15	0.685	1.11	0.680	1.10
40	1.646	1.15	0.704	0.731	1.19				
50	1.567	1.09	0.703	0.738	1.15				
100	1.561	1.09	0.703	0.744	1.15				

* F is the fluorescence correction factor generated by the ZAF program

The corrected set of k-values for Co leads, after the atomic number and absorption correction, to the second concentration profile (open circles in Fig. 7) and a new estimate of 1.3 % Co for C_A^{LB}. This results, in turn in the third profile (open squares). A new calculation based upon a value of 1.13 % for C_A^{LB} eventually yields the final profile which cannot be shown in Fig. 7 because it coincides with the third (see also Table 1). The ultimate value of C_A^{LB} is 1.15 % showing that indeed convergence is obtained.

This is also demonstrated graphically on the left hand side of Fig. 7. As a result an extrapolated boundary concentration of 1.10–1.15 wt% Co will now be obtained, in contrast with the value of 3.5 wt % Co, originally obtained, showing how well our model works in this case! The results for the second example are shown graphically in the top half of Fig. 7. They are somewhat less favourable in that the average end concentration of 2.4 % differs 0.3 % from the real value. Nevertheless a considerable improvement has been achieved after correction as shown by the extrapolated boundary concentration which changes from 5.5 to 2.75 %. Similar results have been calculated for the third example from Fig. 6. Here, after three iterations an average Co-concentration of 4.4 % and an extrapolated boundary concentration of 4.5 % (originally 8.2 %!) are obtained.

The reason for the systematic differences between the corrected and the real concentration must probably be sought in the contribution of continuum fluorescence and, to a lesser extent, in the fact that the use of our model results in some undercorrection as discussed before. If the contribution of continuum fluorescence is calculated as in the case of Fig. 5 has been done and the original k-ratios corrected before the iterations are started, then an average value of 2.25 and an extrapolated value of 2.3 % results for the 2.1 wt % Co alloy.

With the experience that our correction model apparently works so well in the examples discussed so far we have also applied it to many concentration profiles with sloping gradients encountered in practical diffusion problems which constitute a major item in the investigations of our laboratory. It is realised, of course, that an error will be introduced by applying a correction procedure, based on two constant concentrations on both sides of the interface, to a sloping concentration gradient.

It should, however, at the same time be realised that without a distance-dependent fluorescence correction the concentrations measured will invariably be too high as the ZAF program will apply an almost constant F-factor (see e.g. Table 1).

Therefore, it seems quite a reasonable suggestion to assume an average concentration, measured over 5–25 μm from the boundary on both sides of the interface, as initial values of C_A^{LB} and C_A^{LA} to start the iteration procedure with. In fact, there is hardly an alternative to this assumption in practical examples as the presence of a gradient on both sides of the interface involves the assumption of not only four independent concentrations but also about the curvatures. Even if these could be chosen in a justifiable way the calculations would become unduly complex and hardly feasible because e.g. all the mass absorption coefficients in eqs. (6) and (7) would become distance-dependent.

A practical problem with the test of our correction procedure on sloping gradients is that in general there is no longer a check of the results as was the case in previous examples. Actually a number of diffusion experiments in our laboratory are at least partly performed in order to measure phase equilibria as phase diagrams appear not always correct or incomplete. We will now discuss an example of a diffusion couple on which we applied our correction method.

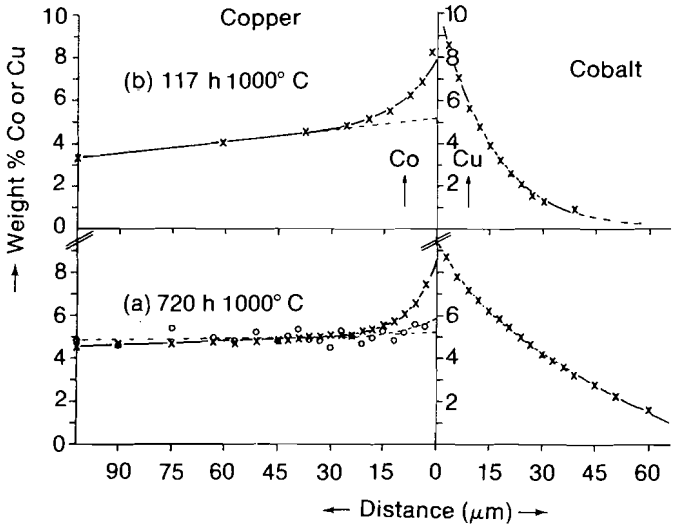

Fig. 8 Concentration profiles for two Co/Cu diffusion couples; top 117 h 1000°C; bottom 720 h 1000°C. The crosses represent the values initially calculated by the ZAF program with k_{Co} and k_{Cu} as input k-ratios. The open circles represent the results of calculations with k_{Cu} only (C_{Co} calculated "by difference").

We selected again the Cu-Co system. Figure 8 shows the concentration profiles measured in two Cu/Co couples heated for 117 and 712 h, respectively, at 1000° C. This gives us at least the opportunity to compare the results which should be the same. According to the phase diagram (*Hansen* 1958) we would expect a boundary concentration of 3.65 wt% Co, which is evidently too low. Simple extrapolation from roughly 25 μm from the boundary would yield a value

of 5.20% Co in both cases. There is, however, no physical justification to do such a thing as it is very well possible that the last part of the profile is curved. Therefore we will consider this value as the absolute minimum for the boundary concentration. On the other hand the extrapolated value of 8.5% is, no doubt, much too high. Fortunately there is another way to get an indication about the real concentration and that is to calculate the Co-concentration by difference in the ZAF program. The results have also been plotted in Fig. 8 (lower half, open circles). Due to the fact that much of the smoothing effect is now lost in the ZAF correction (every iteration starts with normalising the concentrations to 100%) the values shows considerable scatter. Least squares fitting procedures applied to these values indicate that for both profiles most probably a slight curvature upwards is present over the last 10 μm near the boundary (dashed curve). As a result of these considerations we estimate the real boundary concentration to lie between 5.5 and 6 wt % Co. We will now discuss the procedure for couple (a). We will start the iterations with an initial value of 5.62% for C_A^{LB} and a fixed value of 94.00% for C_A^{LA} (6 wt % Cu in Co).

The results for each iteration are shown in Fig. 9 and Table 2, together with the measured original quantities. Also in this case very rapid convergence in two iterations is obtained. The final extrapolated boundary concentration is 6.35 wt % Co which is really not far from our original estimate. Equally pleasing is the fact that the other couple yields a comparable result (6.50%, in 2 iterations). It is evident that, if a correction for continuum fluorescence had been applied, the results could even have been improved. For completeness, we have made a final calculation for both couples based on a value of 5.10 wt % Co for C_A^{LB} which we consider as the absolute minimum average value

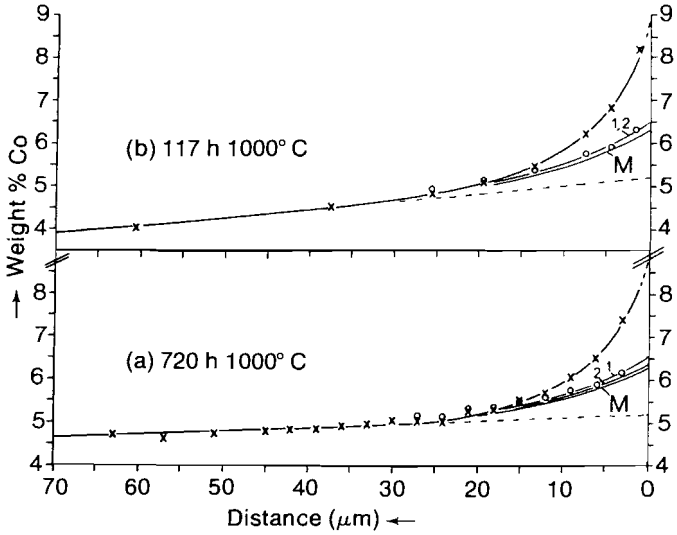

Fig. 9 Results of the iteration process for the two couples of Fig. 8. The crosses represent the original concentrations; the open circles the results of the first iteration.

for C_A^{LB}. The resulting curves, designated by M in Fig. 9, show negligible differences with the results of the last iteration (2). In order to answer the question of how critical the initial values of C_A^{LB} and C_A^{LA} are as well as the area over which C_A^{LB} is averaged we have performed a series of calculations with varying concentrations.

As has briefly been mentioned before, the choice of C_A^{LA} is hardly critical: a variation between 91 and 94.5 wt % Co did not produce a noticeable effect for the last two examples. Regarding the significance of C_A^{LB} it has so far been found that a significantly too high initial value merely increases the number of iterations, the final results being approximately the same.

Table 2 Results for the diffusion couple Cu/Co, annealed for 720 h at 1000° C (see also Figs. 8 and 9).

Measured Values				1st Iter. 5.62%		2nd Iter. 5.50%	
d (μm)	k_{Co}(%)	C_{Co}(wt %)	F	F(d)	C_{Co}(wt %)	F(d)	C_{Co}(wt %)
3	9.995	7.43	0.749	0.623	6.18	0.619	6.14
6	8.832	6.51	0.743	0.673	5.90	0.670	5.87
9	8.238	6.05	0.739	0.703	5.75	0.700	5.72
12	7.781	5.69	0.737	0.723	5.58	0.720	5.56
15	7.579	5.54	0.736	0.736	5.53	0.734	5.52
18	7.279	5.31	0.735	0.745	5.38	0.743	5.37
21	7.211	5.26	0.734	0.751	5.37	0.750	5.37
24	6.878	5.00	0.733	0.757	5.17	0.754	5.15
27	6.946	5.06	0.733	0.759	5.23	0.758	5.22
30	6.970	5.07	0.733	0.761	5.26	0.760	5.26
33	6.843	4.98	0.732				

Table 3 Consequences of different choices for the initial value of C_A^{LB} for couple (a) in Figs. 8 and 9.

C_A^{LB}(wt%Co)	7	6.5	6	5.5	5	4.5	4
distance (μm)			C_{Co} (wt%)				
3	6.57	6.44	6.30	6.14	6.12	5.76	5.53
6	6.17	6.07	5.98	5.87	5.74	5.60	5.43
9	5.95	5.68	5.81	5.72	5.63	5.33	5.39
12	5.74	5.62	5.63	5.56	5.49	5.35	5.30
15	5.66	5.62	5.56	5.51	5.46	5.38	5.31
18	5.49	5.45	5.41	5.37	5.32	5.26	5.20
21	5.47	5.44	5.39	5.36	5.31	5.27	5.21
24	5.24	5.21	5.18	5.15	5.11	5.07	5.04
Average over 5–25 μm	5.67	5.58	5.56	5.51	5.44	5.35	5.27

Table 3 illustrates the consequences of seven different choices for C_A^{LB} for the concentration profile of couple (a) in Fig. 9.

It follows that if we had chosen an initial value of 7% then the average value of C_A^{LB} for the second iteration would have been 5.67% yielding in turn an average value of 5.50% which would result finally in an end value of 5.50% (see also Table 2).

Rather surprising is the observation that for evidently too low initial values of 4.5 and 4% Co for C_A^{LB} (i.e. lower than any measured value far away from the boundary) averages of 5.35 and 5.27% are obtained which would force us to use higher values for the next iterations; thus showing again the desired converging effect. Apparently there is, in this case, really no danger for overshoot as a result of overcorrection. This is due to the fact that for the profiles in Fig. 8 the concentration outside the range over which the effects of fluorescence would be expected, are still high enough to prevent C_A^{LB} from assuming very low (smaller than 1%) values. In these concentration ranges F(d) is not too sensitive for small changes in C_A^{LB} as Tables 1 and 2 show.

The situation is more critical, however, in cases where very low values of C_A^{LB} (smaller than 1%) are involved in connection with a limited area over which diffusion has taken place and C_A is soon approaching zero outside the 25 μm range. When this is the case reducing the area over which the averaging is carried out and/or taking it closer to the boundary seems to be the remedy.

This leads, of course, to a much slower iteration process as was observed in a Cu_2O/Co couple in which after diffusion a layer of Cu adjacent to a CoO layer was developed.

The measured concentration profiles are shown in Fig. 10. The initial boundary concentration seems to lie between 5 and 6 wt% Co. If we now take the average value of C_A^{LB} over only 10 μm from the boundary then 6 iterations are needed (see Fig. 10) with an end value of 1.18% for C_A^{LB}. If we had used the more drastic averaging process previously used, then the first estimate for C_A^{LB} would have been 1.5% yielding 0.85% for the second iteration, leading in turn to 0.65% in the third. As for such low values of C_A^{LB} the value of F(d) becomes extremely sensitive to small variations in C_A^{LB} the danger of overshoot and non-convergence seems realistic. In such cases it is therefore advisable to choose the cautious way and restrict the area over which C_A^{LB} is averaged and/or taking it closer to the boundary.

The final boundary concentration is 1.6 wt% Co which is very close to the value one would expect from the calculations with Co "by difference" (open circles in Fig. 10). At this point it should be noted that in many cases measurements "by difference" are not possible, e.g. in oxide systems where usually the oxygen is already measured "by difference".

Summarizing, it seems to be difficult to give hard general rules for the range over which C_A^{LB} should be averaged or where it should be taken. Especially in cases like the last one should adapt this range to the type of problem in order to obtain smooth convergence from high to lower values of C_A^{LB}. In general one could say that the lower the expected endvalue of C_A^{LB} is, the more caution should be exercised in the choice of C_A^{LB}. Nevertheless, the fact that convergence can be obtained gives us confidence in the results. Moreover, there are many indications that a considerable improvement in the results can be obtained by applying the correction procedure.

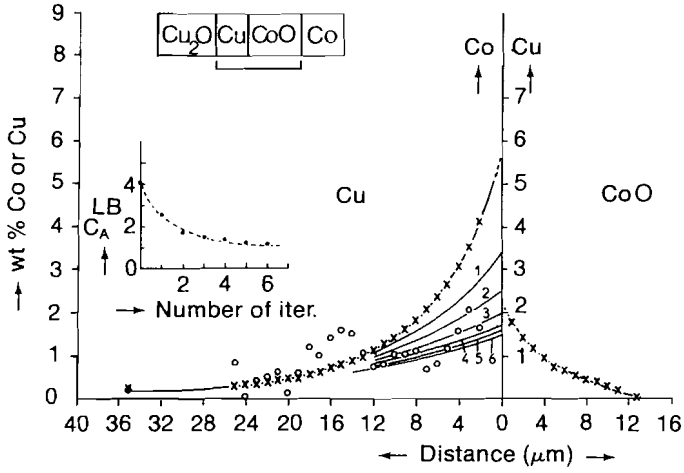

Fig. 10 The iteration procedure applied to a Cu_2O/Co diffusion couple annealed 70 h at 1000°C. The crosses represent the original concentrations; the open circles the Co concentration calculated "by difference".

So far our correction model has not been used yet for the other geometries discussed in the theoretical part of our paper.

It is, however, anticipated that similar procedures can be applied to lamellae, small particles (idealised as hemispheres) and surface layers as long as the parameter d is accurately known and an estimate of C_A^{LA} can be made. In such cases the iteration procedure could be started by choosing the originally measured concentration in the centre of the particle as initial value for C_A^{LB}, calculating F(d), correcting the original k-ratio and converting it into concentration (with disabled fluorescence correction in the ZAF program).

The procedure could then be repeated with the new concentration and so on. It would be especially interesting to test this procedure on particles with varying sizes as are frequently found in two-phased alloys. Ideally this would have to result in about the same concentration for both small and large particles, a concentration which would be equal to the one measured in the largest particles.

The fact that the particles are frequently irregularly shaped is probably outweighed when sufficient particles are available. We have tried to perform such a test in the Cu/Co system but the two-phased alloys produced so far all showed severe coarse segregation after repeated argon-arc melting, which prevented equilibrium being attained even after very long annealing treatments at 1000° C. This has also eliminated the possibility of a comparison between the equilibrium concentrations measured in very large particles and the values obtained through our correction procedure in the diffusion couples of Figs. 8 and 9. At the moment experimental work on this effect is still in progress as is the search for other suitable systems to test for example the equations for (epitaxial) layers on substrates.

Summary

A correction procedure is proposed to correct for the effects of characteristic fluorescence in electron probe micro-analysis near phase boundaries. To this end a number of equations have been derived for various geometries which are frequently encountered in practice. These include two metals or alloys, separated by a straight boundary either parallel (diffusion couple, lamella) or perpendicular to the incident electron beam (thin layer on substrate) as well as (idealised) small particles in a matrix.

Some of these equations have been tested in practice in couples formed by either pure metals or homogeneous alloys and it has been shown that they are well capable of predicting the apparent concentration of the element suffering from secondary excitation as a function distance from the boundary.

Based on these equations an iterative correction procedure is proposed for application to sloping concentration profiles.

The initial microprobe measurements are hereby used to obtain an estimate of the average concentrations over the relevant areas on both sides of the interface. These are then used to calculate a correction factor as a function of distance to correct the measured k-ratio of the excited element with. The usual ZAF correction, with disabled fluorescence correction, will then yield new concentration values after which the procedure is repeated until convergence is obtained.

The procedure is illustrated on some practical examples and the factors concerning the choice of the initial estimates are discussed.

References

Castaing R, Descamps J: The physical basis of quantitative analysis by x-ray spectrography. J Phys Radium 16, 304–317 (1955)

Green M: Angular distribution of characteristic x-radiation and its origin within a solid target. Proc Phys Soc 83, 435–451 (1964)

Green M, Cosslett VE: The efficiency of production of characteristic x-radiation in thick targets of a pure element. Proc Phys Soc 78, 1206–1214 (1961)

Hansen M: Constitution of binary alloys. 2nd Ed. McGraw-Hill Book Comp., New York 1958

Henoc J, Maurice F, Zemskoff A: Phénomènes de fluorescence aux limites de phases. Vth Intern Congress on X-ray Optics and Microanalysis (eds G Möllenstedt, KH Gaukler), Springer, Berlin–Göttingen–Heidelberg 1968, 187–192

Maurice F, Seguin R, Henoc J: Phénomènes de fluorescence dans les couples de diffusion. IVe Congrès International sur l'Optique des Rayons et la Microanalyse, Orsay (1965), 357–364

Reed SJB: Characteristic fluorescence corrections in electron probe microanalysis. Brit J Appl Phys 16, 913–926 (1965)

Reed SJB, Long JVP: Electron-probe measurements near phase boundaries. 3rd Int Symp on X-ray Optics and X-ray Microanalysis, Stanford (1962), (eds HH Pattee, VE Cosslett, A Engström), Academic Press, New York 1963, pp 317–327

Reed SJB: Electron Microprobe Analysis Cambridge University Press, Cambridge 1975